Developmental Cell
Short Article

Drosophila Maelstrom Ensures Proper Germline Stem Cell Lineage Differentiation by Repressing *microRNA-7*

Jun Wei Pek,[1] Ai Khim Lim,[1] and Toshie Kai[1,*]
[1]Department of Biological Sciences and Temasek Lifesciences Laboratory, Germline Biology Laboratory, 1 Research Link, The National University of Singapore, Singapore 117604
*Correspondence: toshie@tll.org.sg
DOI 10.1016/j.devcel.2009.07.017

SUMMARY

Nuage is a germline-unique perinuclear structure conserved throughout the animal kingdom. Maelstrom (Mael) is an unusual *nuage* component, as it is also found in the nucleus. Mael contains a High Mobility Group box, known to mediate DNA binding. We show that Mael nuclear function is required for proper differentiation in the *Drosophila* germline stem cell (GSC) lineage. In *mael* mutant testes, transit-amplifying cysts fail to differentiate into primary spermatocytes, instead breaking down into ectopic GSCs and smaller cysts, due to a depletion of Bag-of-marbles (Bam) protein. Mael regulates Bam via repression of *miR-7*. Mael binds the *miR-7* promoter and is required for the local accumulation of HP1 and H3K9me3. *miR-7* targets *bam* directly at its 3′UTR, and a reduction in *miR-7* expression can rescue germline differentiation defects found in *mael* mutants by alleviating Bam repression. We propose that Mael ensures proper differentiation in the GSC lineage by repressing *miR-7.*

INTRODUCTION

Drosophila melanogaster spermatogenesis is an excellent model to study cell differentiation. The germline stem cell (GSC) lineage was shown to be able to revert into GSCs for regeneration (Brawley and Matunis, 2004; Cheng et al., 2008; Kai and Spradling, 2004). Therefore, it is important that differentiation of the GSC lineage is appropriately maintained and regulated for proper gametogenesis and to prevent tumor formation (Fuller, 1993).

Animal germline cells contain a perinuclear structure found at the cytoplasmic face of the nuclear envelope called the *nuage* (Eddy, 1975), which is also known as P granules in *C. elegans* and chromatoid body in mammals (Kotaja and Sassone-Corsi, 2007). Some proteins that localize to the *nuage* have been shown to be required for silencing of retrotransposons and *stellate* in the *Drosophila* germline via the piRNA pathway (Klattenhoff and Theurkauf, 2008). One of those, Maelstrom (Mael), is unusual in that it has been shown to localize to the nucleus, as well as to the *nuage* (Findley et al., 2003). Mael contains a High Mobility Group (HMG) box (Findley et al., 2003), suggesting the possibility of an unknown nuclear function.

The mouse homolog of Mael localizes to the *nuage* (Costa et al., 2006; Soper et al., 2008), where it exists as a complex with Mili and Miwi (Kotaja and Sassone-Corsi, 2007). Recently, mouse *mael* has been shown to be required for retrotransposon repression and spermatogenesis (Soper et al., 2008), which suggests a conservation of *mael* function(s) among different species. Furthermore, mouse Mael was found to interact with chromatin-remodeling factor SNF5 and chromatin-associated protein SIN3B, suggesting a nuclear function in controlling gene expression (Costa et al., 2006).

Here we report a nuclear function for Mael which ensures proper GSC lineage differentiation in *Drosophila melanogaster*. Mael represses the expression of *miR-7*, which targets *bag-of-marbles* (*bam*) via its 3′UTR. Overexpression of *miR-7* in *mael* mutant testes resulted in a downregulation of Bam, leading to a differentiation defect. Therefore, we propose that Mael ensures proper GSC lineage differentiation by repressing *miR-7*.

RESULTS

Mael Is Required for GSC Lineage Differentiation

To examine the function of *mael*, we used a loss-of-function allele, $mael^{M391}$ (Findley et al., 2003). In *Drosophila* testes, GSCs lie directly adjacent the hub with spherical fusomes, germline-specific cytoplasmic structures (de Cuevas and Spradling, 1998). They divide asymmetrically to give rise to themselves and differentiating gonialblasts (GBs), which do not contact the hub but contain spherical fusomes. GBs undergo four rounds of synchronous mitotic division to form cysts of spermatogonia interconnected by fusomes, which branch during cyst formation (Figure 1A; de Cuevas and Spradling, 1998). The 16-cell cysts then exit the mitotic cycle and enter meiosis (Fuller, 1993; Fuller and Spradling, 2007).

We observed massive accumulation of early germ cells in 8-day-old *mael* mutant testes, but not in controls (Figures 1B and 1C), a phenotype that was rescued by expressing *FLAG-mael* with the germline driver *NGT40* (Figure 1D; Tracey et al., 2000). This phenotype is unique to *mael*, as mutants of other *nuage* component genes such as *aubergine* (*aub*) did not exhibit such a defect (see Figure S1 available online). The defect was not due to a reduction in cell death, as control and *mael* mutants had similar percentages of apoptotic germ cells (Figure S2A). We did

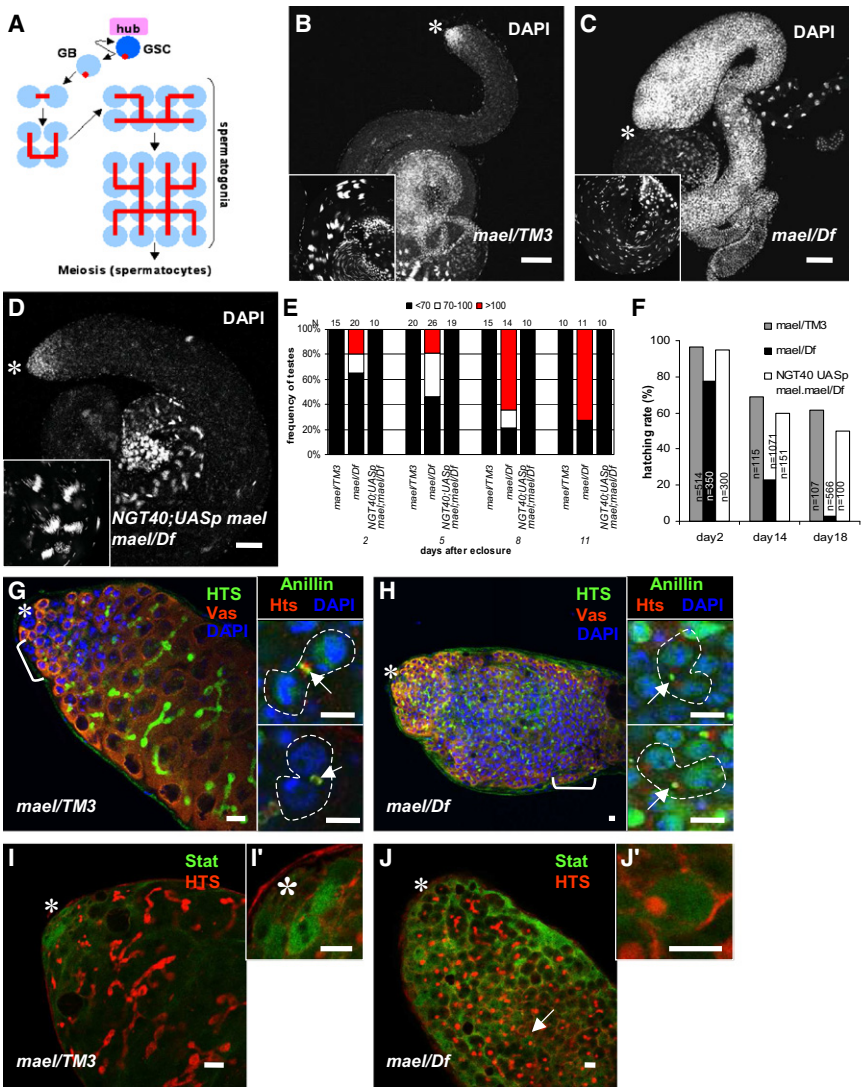

Figure 1. Mael Is Required for GSC Lineage Differentiation

(A) Schematic diagram showing the GSC lineage in the *Drosophila* testes. Germline cells are in blue, and fusomes in red.

(B–E) Day 8 *mael/TM3* (B), *mael/Df* (C), and *NGT40; UASp-mael mael/Df* (D) testes stained with DAPI. Scale bar: 150 μm. Insets show sperm bundles.

(E) The percentage of testes with the indicated number of spermatogonial cysts at different days post eclosure.

(F) The hatching rate of embryos from the mating of *mael/TM3*, *mael/Df*, or *NGT40;UASp-mael mael/Df* males crossed with virgin wild-type females.

(G and H) *mael/TM3* (G) and *mael/Df* (H) testes stained for HTS (green), Vas (red), and DAPI (blue). Brackets indicate regions that were magnified in insets stained for Anillin (green), HTS (red), and DAPI (blue). Arrows indicate ring canals and dotted lines mark cysts. Scale bar: 50 μm.

(I and J) *mael/TM3* (I) and *mael/Df* (J) testes stained for Stat (green) and HTS (red). The arrow indicates Stat-positive single cells magnified in (I′) and (J′), respectively. Scale bar: 50 μm.

not observe any GSC maintenance defect when we overexpressed *FLAG-mael* in the germline (data not shown), suggesting that overexpression of Mael does not force GSCs to differentiate.

Accumulation of early germ cells became more severe as the flies aged (Figure 1E), accompanied by a drastic drop in fertility (Figure 1F) and fewer sperm bundles (Figures 1B and 1C). *mael* mutant spermatogonia underwent more than the usual four rounds of mitotic cell division to form cysts containing more than 16 cells, such as 32-cell cysts (Figure S2B), with 16-cell cysts synchronously staining positive with anti-PH3, which was never seen in controls (Figure S2C).

Beside undergoing more than the usual four rounds of division to form 32-cell cysts, *mael* mutant testes had cysts harboring abnormal numbers of cyst cells instead of the normal 2, 4, 8, and 16, and many 2-cell cysts and single cells that mingled with larger cysts of abnormal cell number (data not shown). These mutant cysts might have dedifferentiated into GSC-like cells by breaking down, as reported previously (Brawley and Matunis, 2004; Kai and Spradling, 2004). To look for breakdown of cysts, we examined the integrity of ring canals, cytoplasmic bridges between cyst cells, which remain open in differentiating cysts due to incomplete cytokinesis (Pepling et al., 1999). When cysts dedifferentiate, they start to break down by closing the ring canals and pinching off the fusomes, leaving ring canal remnants (Brawley and Matunis, 2004; Kai and Spradling, 2004). In control testes, ring canals visualized with anti-anillin antibody were intact in mitotically dividing cysts (Figure 1G, arrows). However in *mael* mutants, we observed single cells and cysts with spherical fusomes and remnants caused by the closure of ring canals (Figure 1H, arrows). We also observed similar ring canal closure in *mael* mutant ovaries (Figure S3), suggesting that cysts were breaking down in *mael* mutant testes and ovaries. Germline-soma interactions have been shown to promote GSC lineage differentiation (Kiger et al., 2000; Sarkar et al., 2007; Tran et al., 2000). We therefore checked if the differentiation defects seen in *mael* mutant testes were due to an encapsulation defect. Using anti-armadillo, which stains the hub and somatic cyst cells, we did not observe any defects in the architecture of the somatic cyst cells (Figures S2D and S2E), suggesting that differentiation defects seen in *mael* mutants were not due to defective encapsulation by somatic cells.

We verified that the ectopic single cells in *mael* mutant testes were GSC-like cells by using the male GSC marker, Stat (Singh and Hou, 2008). In control testes, only GSCs lying beside the hub were positive for Stat (Figure 1I). In *mael* mutant testes, GSC-like cells, which were positive for Stat, were seen both near and away from the apex (Figure 1J, arrows). We observed single dividing germline cells with round fusomes stained positive for BrdU and PH3 away from the hub in *mael* mutant testes,

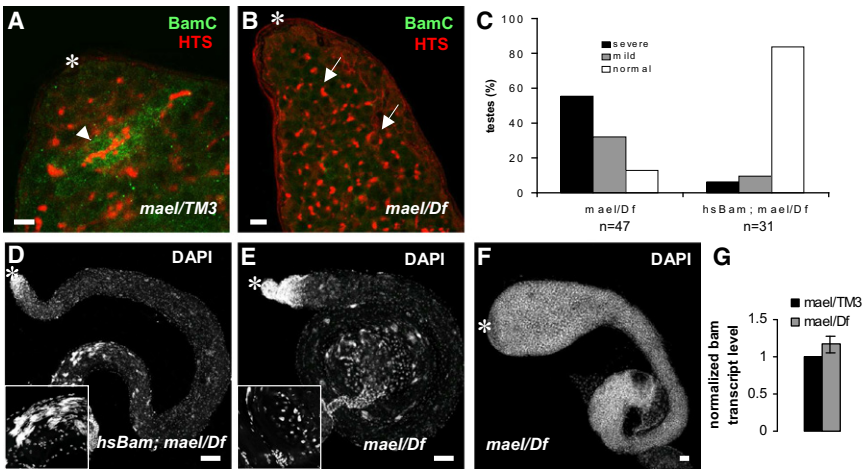

Figure 2. The Differentiation Defect in *mael* Mutants Is Due to a Depletion of Bam

(A and B) *mael/TM3* (A) and *mael/Df* (B) testes stained for BamC (green) and HTS (red). Scale bar: 50 μm. Arrowheads show Bam-positive cysts in the control, whereas arrows show BamC-negative cysts that have broken down in *mael* mutant testis.

(C) The percentages of *mael* mutant testes showing normal, mild, and severe differentiation defects as shown in D–F either with or without *bam* overexpression.

(D–F) Testes of the indicated genotype were stained with DAPI. *mael* mutant testes with *bam* overexpression showing normal morphology (D) and without *bam* overexpression showing mild (E) and severe (F) differentiation defects. Scale bar: 50 μm. Insets show sperm bundles.

(G) Chart showing the relative normalized level of *bam* transcripts in *mael/TM3* and *mael/Df*. n=3. All error bars represent standard deviation.

indicating active mitosis of germline cells away from the niche (Figures S2F and S2G). Therefore, our results suggest that *mael* is required to ensure proper differentiation of the GSC lineage. In *mael* mutants, although initial differentiation of GBs into cysts occur, differentiating cysts cannot be maintained and break down into smaller cysts and GSC-like cells, which continue to divide mitotically, eventually leading to a drastic increase in severity of the phenotype over time.

The Differentiation Defect in *mael* Mutants Is Due to a Depletion of Bam

Since the differentiation defect seen in the *mael* mutant was similar to that reported for *bam* mutants (Gonczy et al., 1997; McKearin and Spradling, 1990), we asked if cytoplasmic Bam expression was affected in *mael* mutant testes. In control testes, Bam protein was detected in 2- to 16-cell cysts but not in the GSCs, GBs, and primary spermatocytes (Figure 2A). In *mael* mutants, Bam expression was low or not detected in ectopic GSCs and smaller cysts that had broken down from larger cysts (Figure 2B, arrows), suggesting that in *mael* mutants, expression of Bam protein is not enough to maintain differentiation, leading to the subsequent breakdown of cysts. To test this hypothesis, we overexpressed *bam* in 8-day-old *mael* mutant testes by inducing *bam* transgene expression using the heat-shock promoter. The differentiation defects in *mael* mutants (Figures 2E and 2F) were rescued by Bam expression (Figures 2C and 2D). Thus, we conclude that the differentiation defect in *mael* mutants is due to a reduction of Bam expression.

Mael Represses *miR-7* Expression

Although we observed a reduction of Bam protein expression in *mael* mutants, we failed to detect any change in *bam* transcript levels (Figure 2G), suggesting that Bam translation was perturbed in *mael* mutants. Recently, it was shown that misexpression of miRNAs could lead to germline defects in *Drosophila* ovaries (Neumüller et al., 2008). We wondered if the perturbation of the Bam protein level in *mael* mutant testes could be mediated by miRNAs. In support of this idea, we observed a partial rescue of the differentiation defect caused by the *mael* mutant as a consequence of reducing *loquacious* or *dicer-1* activity, to lower the capacity for miRNA biogenesis (Figure 3A; 71 ± 30 cysts in *mael/Df* versus 31 ± 5 cysts in *dcr-1/+;mael/Df* and 36 ± 6 cysts in *loqs/+;mael/Df*; see Experimental Procedures for cyst quantification). This suggests that the differentiation defect in the *mael* mutant is mediated by excessive miRNA activity.

Searching miRbase identified *miR-7*, *306*, *275*, and *317* as miRNAs that might target *bam* (Griffiths-Jones, 2004). Using real-time RT-PCR, we examined the levels of these four miRNAs and *bantam*, which was proposed to function in GSC self-renewal in ovaries (Neumüller et al., 2008). *miR-7* showed a 2-fold upregulation, while *miR-306* and *miR-317* showed modest upregulation, in the *mael* mutant testes (Figure 3B). *bantam* levels were unchanged, and *miR-278* was not detectable in either control or mutant testes (Figure 3B). We chose to look more closely into *miR-7* for several reasons. First, *miR-7* was most significantly upregulated in *mael* mutants. Second, *miR-7* expression was found to be low or undetected in wild-type ovaries and testes (Aravin et al., 2003; Neumüller et al., 2008), suggesting a need for it to be repressed. Third, the *miR-7* promoter is characterized and was shown to be spatially and temporally regulated during photoreceptor development and embryogenesis (Aboobaker et al., 2005; Li and Carthew, 2005). Finally, the *miR-7* mutant is available, making genetic studies possible. Indeed, removing one copy of *miR-7* in the *mael* mutant background partially suppressed the differentiation defect (Figures 3A and 3C; 71 ± 30 cysts in *mael/Df* versus 43 ± 6 cysts in *miR-7/+;mael/Df*). In contrast, the differentiation defect was not suppressed when we removed one copy of *bancal* or *bantam* in the *mael* mutant background (Figure 3A and Figure S4), further confirming a specific genetic interaction between *miR-7* and *mael*.

The *nuage* has been proposed to be involved in piRNA biogenesis (Brennecke et al., 2007; Lim and Kai, 2007; Pane et al., 2007). *mael*, as well as *aub*, are required for retrotransposon silencing in the *Drosophila* testes and ovaries (Figure S2; Lim and Kai, 2007). However, no change in *miR-7* level was detected in *aub* mutants (Figure S5), suggesting that upregulation of

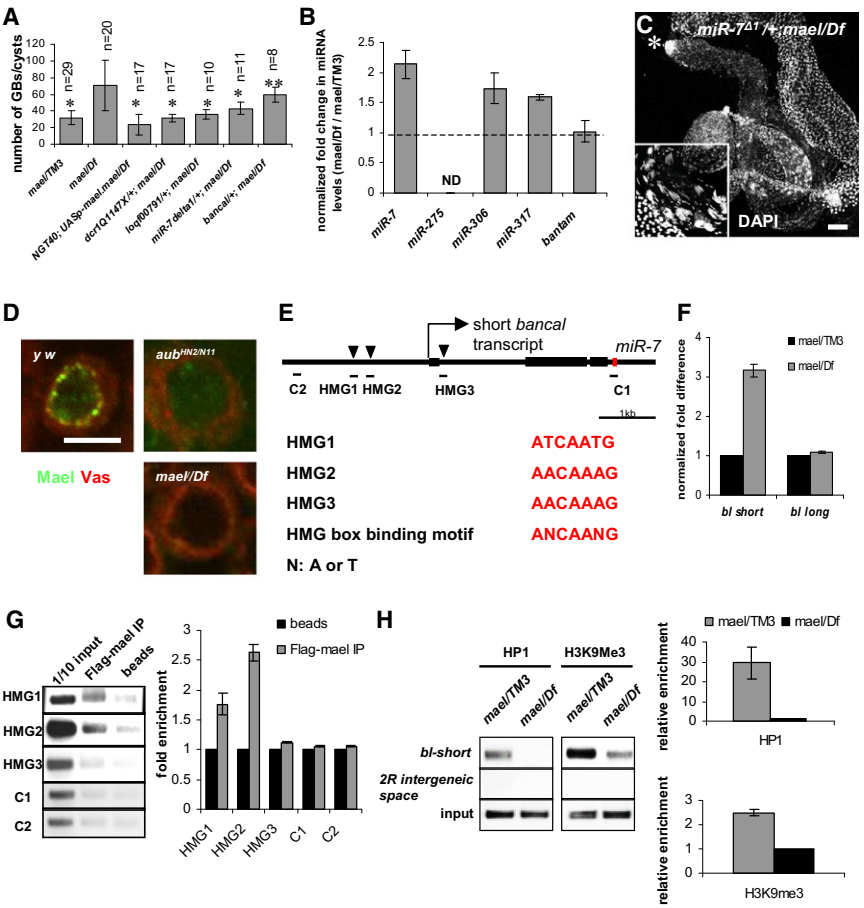

Figure 3. Mael Represses *miR-7* Expression

(A) Chart showing mean number of GBs/cysts of the indicated genotype. Significant difference compared to *mael/Df*, *p < 0.01, two-tailed t test; significant difference compared to *miR-7*$^{\Delta 1}$*/+; mael/Df*, **p < 0.001, two-tailed t test.

(B) Chart showing fold change (*mael/Df* over *mael/TM3*) in the levels of each miRNA.

(C) *miR-7*$^{\Delta 1}$*/+;mael/Df* mutant testes stained with DAPI. Inset shows sperm bundles. Scale bar: 150 μm.

(D) Localization of Mael in *aub* and *mael* mutants. Mael, green; Vas, red. Scale bar: 50 μm.

(E) *miR-7* locus showing three putative HMG-box binding motifs (HMG1, -2, and -3) marked by arrowheads. Black boxes denote exons. C1 and C2 are two regions without HMG-box binding motifs located ~2.8 kb downstream and upstream of the transcription start site respectively. Regions amplified by PCR detecting HMG1, -2, -3, C1, and C2 are indicated by horizontal lines.

(F) Real-time PCR results for *bancal (bl)* short and long transcripts in *mael/TM3* and *mael/Df*. n = 3.

(G) PCR and quantification of ChIP products normalized against the input using primers designed to amplify indicated regions. n = 3.

(H) PCR of ChIP products pulled down by anti-HP1 and anti-H3K9me3 in *mael/TM3* and *mael/Df* using primers designed to amplify promoter region of *miR-7*. n = 3. All error bars represent standard deviation.

miR-7 in *mael* mutant testis is not due to compromised piRNA production. In *aub* mutant testes, Mael localization to *nuage* was disrupted, while its localization to the nucleus was unaffected (Figure 3D). The nuclear staining of Mael in *aub* mutants was specific, as it was not seen in the *mael* mutants (Figure 3D). These results suggest that Mael has an additional nuclear function, to repress *miR-7* via a piRNA-independent pathway. Like many HMG-box proteins, Mael could regulate transcription of *miR-7*. The *miR-7* locus is in the intron of the *bancal* gene and is believed to be driven by a distinct internal promoter that gives rise to a short *bancal* isoform, which is the primary *miR-7* transcript (Figure 3E; Aboobaker et al., 2005; Li and Carthew, 2005). Using real-time PCR, we detected an ~5-fold upregulation of the short isoform encoding the primary *miR-7* transcript, but not the long isoform encoding the Bancal protein, in *mael* mutant testes (Figure 3F). No change in the short or long isoforms was detected in *aub* mutant testes (Figure S5).

HMG-box proteins have been shown to regulate gene expression by binding to HMG-box binding motifs in the promoter/regulatory regions of the genes that they regulate (Beest et al., 2000). We examined the 3 kb genomic sequence upstream of the *bancal* short isoform encoding *miR-7* as well as the entire *bancal* short isoform genomic sequence and identified three HMG-box binding motifs, HMG1, -2, and -3 (Figure 3E). We examined whether Mael binds to these motifs by chromatin immunoprecipitation (ChIP). Immunoprecipitates with anti-FLAG from ovary extract expressing *FLAG-mael* driven by *nanos-Gal4*, which fully rescued the differentiation defect in *mael* mutant ovaries (Figures S3E and S3F), were subjected to PCR. We detected significant enrichment for two HMG-box binding sequences upstream of the *miR-7* transcription start site (Figure 3G), but not for the one located downstream of the *miR-7* transcription start site, or to two control regions devoid of HMG-box motifs, C1 and C2 (Figure 3G). Also by ChIP analysis, we observed that binding of Heterochromatin Protein 1a (HP1a) to *miR-7* promoter was reduced in *mael* mutants, accompanied by a reduction of trimethylated histone3-lysine9 (H3K9me3) in the same region (Figure 3H). Taken together, our data suggest that Mael binds to the *miR-7* promoter region and is required for local accumulation of HP1 and H3K9me3 to repress *miR-7* expression via an epigenetic mechanism.

miR-7 Represses Bam Expression

The *miR-7* target site in the *bam* 3′UTR is only found in the *melanogaster* subgroup, with a single thymine to adenine base change in *D. simulans* and *D. sechellia* (Figure S6), suggesting that the site emerged very recently during evolution and it is diverging in the closest relatives of *D. simulans* and *D. sechellia*. Furthermore, the site contains two G:U base pairs, making it unusual compared to normal miRNA "seeds" (Figure 4A; Brennecke et al., 2005). We therefore tested whether the *miR-7* target site is functional in vivo. We generated sensor lines containing

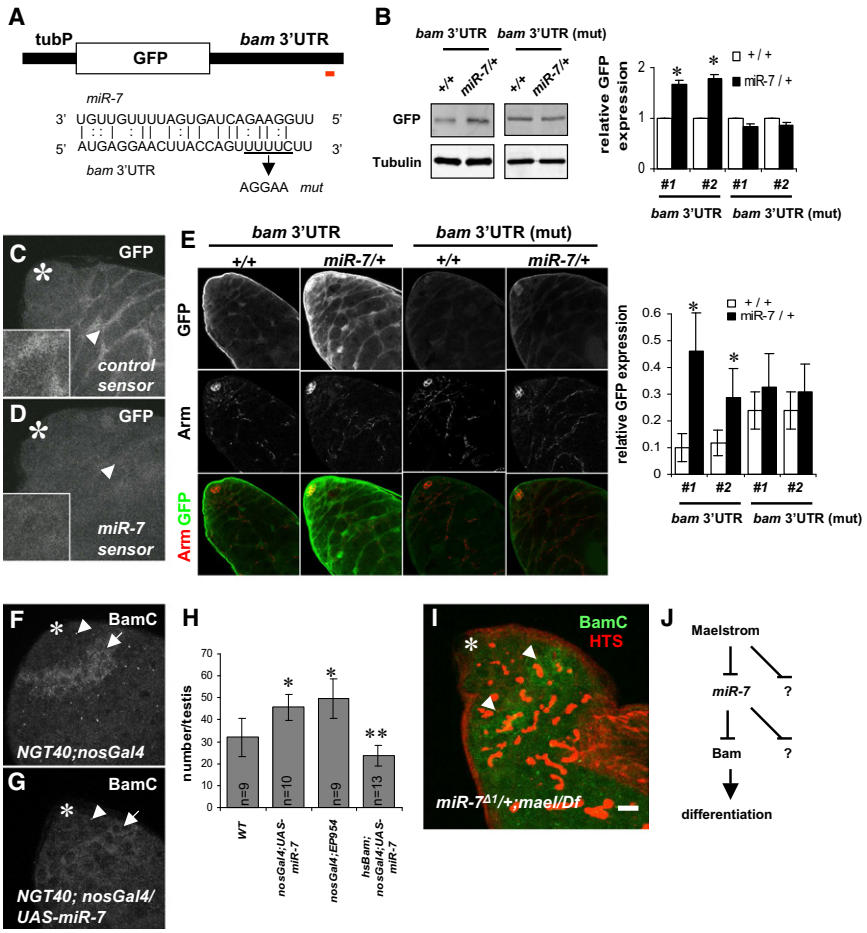

Figure 4. *miR-7* Represses Bam Expression

(A) Schematic diagram (not drawn to scale) of the tubulin promoter-GFP-*bam* 3′UTR reporter construct. The potential *miR-7* binding site lies in the *bam* 3′UTR is indicated by red bar. The sequence with the *miR-7* binding site and the mutated nucleotides used in (D) are shown below.

(B) Western blots and chart showing GFP protein expression from tubulin promoter-GFP with WT and mutated *bam* 3′UTR in +/+ and *miR-7*/+ backgrounds. Two independent transgenic lines were examined each for WT and mutated 3′UTR. GFP expression was normalized against tubulin. Significant difference compared to +/+, *$p < 0.001$, two-tailed t test. n = 3 independent experiments.

(C and D) GFP signals in the somatic cyst cells of control (C) and *miR-7* sensor line (D). Arrowheads point to somatic cyst cells magnified in insets.

(E) Representative images of testes and chart showing GFP signals from reporters used in (B). n = 8–10 testes for each genotype. GFP signals were normalized against Armadillo signals. Significant difference compared to +/+, *$p < 0.001$, two-tailed t test.

(F and G) *NGT40;nosGal4* (F) and *NGT40;nosGal4/UAS-miR-7* (G) testes stained for BamC. Arrowheads point to GSCs/GBs, and arrows point to regions where spermatogonia reside.

(H) The mean number of spermatogonial cysts in *wild-type*, *NGT40;nosGal4/UAS-miR-7*, *NGT40/EP954;nosGal4*, and *hsBam;nosGal4/UAS-miR-7*. Significant difference compared to wild-type, *$p < 0.05$, two-tailed t test; significant difference compared to *NGT40;nosGal4/UAS-miR-7*, **$p < 0.05$, two-tailed t test. All error bars represent standard deviation.

(I) *miR-7$^{\Delta 1}$/+;mael/Df* mutant testes stained for BamC (green) and HTS (red). Arrowheads indicate BamC-positive cysts. Scale bar: 50 μm.

(J) Proposed model in which Mael represses the expression of *miR-7*, where *miR-7* represses the expression of Bam required for differentiation.

bam 3′UTR or the same 3′UTR with the *miR-7* sites mutated, placed downstream of GFP under the tubulin promoter (Figure 4A). Quantitative western blot analysis showed that GFP expression in the testes increased when the *miR-7* level was lowered for the intact 3′UTR, but not the mutated ones (Figure 4B). We confirmed our results in the somatic cyst cells, where the endogenous activity of *miR-7* is enough to repress the GFP expression from the *miR-7* sensor line but not the control sensor devoid of *miR-7* target sites (Figures 4C and 4D; Stark et al., 2003). Using the *bam* 3′UTR sensor lines, we observed that when *miR-7* level is lowered, GFP expression in somatic cyst cells was upregulated for the intact 3′UTR but not the mutated ones (Figure 4E). Taken together, our data confirm that *miR-7* directly target *bam* 3′UTR at the predicted seed region.

We investigated whether overexpression of *miR-7* in the germline could reduce Bam protein levels. *EP954* has the P element inserted 52 base pairs upstream of the *miR-7* transcription start site, which allows Gal4-inducible transcription of the sequences flanking the P element (Rorth et al., 1998). When *miR-7* was overexpressed by driving *UAS-miR-7* and *EP954* with *nanos-Gal4*, we observed a downregulation of Bam protein compared to that in the controls (Figures 4F and 4G). We also observed an increase in the number of spermatogonial cysts when *miR-7* was overexpressed (Figure 4H; 32 ± 8 cysts in controls versus 46 ± 6 cysts in *NGT40;nos-Gal4/UAS-miR-7*; 50 ± 9 cysts in *NGT40/EP954;nosGal4*). This high number of spermatogonial cysts was reduced to 24 ± 5 by expression of *bam* (Figure 4H), further confirming that overexpression of *miR-7* can inhibit differentiation by repressing Bam expression. Importantly, removing one copy of *miR-7* in the *mael* mutant background restored the level of Bam protein to that seen in controls, and the rescue of the differentiation defect was discernible by the restoration of cysts with branched fusomes (Figure 4I, compare to Figure 2A). We conclude that the differentiation defect seen in *mael* mutants is mediated, at least in part, by overexpression of *miR-7*, which suppresses Bam expression.

DISCUSSION

GSC maintenance and division are controlled by the miRNA pathway (Forstemann et al., 2005; Hatfield et al., 2005; Jin and

Xie, 2007; Park et al., 2007); however, little is known about how miRNAs regulate the GSC lineage. We have shown that Mael is required for male GSC lineage differentiation by repressing *miR-7*, thus alleviating the repression of Bam by *miR-7* (Figure 4J). A previous study had shown that Mei-P26 restricts growth and proliferation in the ovarian cysts by inhibiting the miRNA pathway. Mei-P26 interacts with Ago1 and possibly regulates the RISC complex (Neumüller et al., 2008). Together with our data, it appears that miRNAs are tightly controlled during different stages of their biogenesis in the GSC lineage, and hence a complex network of miRNA regulation operates in the germline.

miRNAs show extensive expression patterns and can be regulated both at the transcriptional and posttranscriptional levels (Bushati and Cohen, 2007). In the *Drosophila* eye, *miR-7* transcription is regulated by Yan, which is in turn regulated by the EGFR signaling pathway (Li and Carthew, 2005). Our data reveal regulation of *miR-7* by Mael in the germline. Mouse Mael has been shown to interact with Sin3B (a component of the histone deacetylase complex) and SNF5 (a SWI/SNF chromatin-remodeling complex) (Costa et al., 2006), implying that Mael may regulate germline gene expression via an epigenetic mechanism. Indeed, we show a local accumulation of HP1 and H3K9me3 at the promoter region of *miR-7* in a *mael*-dependent manner. Therefore, in the *Drosophila* germline, *mael* may function as a transcriptional regulator for tissue-specific regulation of genes and miRNAs including *miR-7.*

Our work sheds light on a possible mechanism by which *Drosophila* might replenish their GSCs by regulating *mael* to induce dedifferentiation. In mammals, breakdown of spermatogonia to replenish GSCs has been reported (Nakagawa et al., 2007). Breakdown of differentiating cysts to GSCs have also been shown in the *Drosophila* germline (Brawley and Matunis, 2004; Cheng et al., 2008; Kai and Spradling, 2004). Unlike in GSCs, where *bam* is transcriptionally silenced by the BMP signaling pathway (Chen and McKearin, 2003; Song et al., 2004), in differentiating cysts, where transcription of *bam* takes place, *bam* can be regulated posttranscriptionally via miRNAs. Since depletion of Bam in differentiating cysts can cause dedifferentiation into GSCs (Kai and Spradling, 2004), *mael* regulation of Bam via *miR-7* is a potential mechanism by which to induce cyst dedifferentiation into GSCs in times of need. miRNAs can facilitate the process by inhibiting translation of Bam while the system changes its transcriptional output. Although the HMG-binding motif, which showed significant enrichment by Mael ChIP, as well as the *miR-7* target site in the *bam* 3′UTR are conserved only in the *melanogaster* subgroup (Figure S6), similar mechanisms involving regulation of miRNAs might have evolved independently in other species.

It was shown that activation of Stat in somatic cyst cells is sufficient to cause GSCs to self-renew outside their niche (Leatherman and DiNardo, 2008). Although we observed an increase in Stat in the somatic cells in *mael* mutant testes (Figure 1I and 1J), we believe that Mael functions primarily in the germline, as the *mael* mutants can be rescued by driving Flag-*mael* transgene under the germline-specific driver, *NGT40-Gal4* (Figures 1D–1F). Therefore, the activation of Stat in somatic cells could be an indirect consequence of signaling from dedifferentiating germline cysts to the somatic cells to establish a microenvironment suitable to maintain ectopic GSCs. However, we could not totally exclude the possibility that Mael has a role in somatic cells.

In conclusion, we have shown that Mael ensures proper differentiation of the GSC lineage by repressing *miR-7*. Understanding the mechanism by which Mael regulates gene expression and the link between Mael and the mechanism of cellular dedifferentiation would be outstanding subjects for future studies.

EXPERIMENTAL PROCEDURES

Fly Strains

The wild-type *Drosophila melanogaster* strain used in this study was *y w*, unless otherwise stated. The mutant alleles used were $aub^{HN2/N11}$, $mael^{M391}/Df(3L)79E\text{-}F$, $dcr\text{-}1^{Q1147X}$, w^{1118}; *P[w+,hsp70 bam+] 11d* (Ohlstein and McKearin, 1997), *control sensor* (Brennecke et al., 2003), *miR-7 sensor* (Stark et al., 2003), $miR\text{-}7^{\Delta 1}$ (Li and Carthew, 2005), $bancal^{k08305}/CyO$ (Kyoto stock center), $loqs^{f00791}$, *UAS-miR-7* (Li and Carthew, 2005), and *EP954* (Li and Carthew, 2005). *hs-bam;mael/Df* flies were heat-shocked at 37°C for 1 hr at 12 hr intervals 6 times and dissected 12 hr after the last heat shock. *hs-bam; nosGal4;UAS-miR-7* flies were heat-shocked at 37°C for 1 hr at 12 hr interval 2 times and dissected 12 hr after last heat shock. *FLAG-mael* and *tubP-GFP-3′UTR* transgenic flies were generated as described previously (Lim and Kai, 2007). Full-length *mael* coding sequence was amplified using *cacc-Mael-1Fw* and *Mael-2Rv* (Table S1) with cDNA LD20229 as a template, and then cloned into pPFW (The *Drosophila* Gateway Vector Collection) in accordance with the manufacturer's protocol. The *bam* 3′UTR was amplified by PCR from *bam* cDNA and cloned into tubulin-EGFP.

Generation of Antibody

Guinea pig anti-Mael was raised against GST-tagged Mael (aa 137 to the end). The portion of *mael* was amplified and cloned into pDEST15, and GST-tagged peptides were purified as in the manufacturer's protocol.

Immunostaining

Testes from males were dissected, stained, and mounted as described previously (Lim and Kai, 2007). The following primary antibodies were used: rabbit anti-Vas (1:200, P. Lasko), guinea pig anti-Mael (1:500), mouse anti-HTS monoclonal 1B1 (1:20, DSHB), mouse anti-Arm (1:100, DSHB), guinea pig anti-BamC (1:200, D. McKearin), rabbit anti-PH3 (1:200, Upstate Biotechnology), rabbit anti-Anillin (1:200, C.M. Field), mouse anti-Stat (1:200, S. Hou), and rabbit anti-GFP (1:200, AbCam). ApopTag staining was performed as described previously (Kai and Spradling, 2003). Secondary antibodies used were Alexa-fluor 488-, 555-, and 633-congugated goat anti-mouse, anti-rat, anti-rabbit, and anti-guinea pig IgG (1:200) (Molecular Probes). DNA was visualized by DAPI (4′,6-diamidino-2-phenylindole). Images were acquired using either Carl Zeiss LSM 510 or 5 Exciter confocal microscopes. Quantification of signal intensity was done using ImageJ software.

Quantification of Cysts

GBs and spermatogonial cysts (interconnected germline cells) were collectively referred to as "cysts" unless otherwise stated. Spermatogonia were identified by their dense nuclear staining by DAPI, and cyst clusters were visualized by HTS staining.

Real-Time and Two-Step RT-PCR

Real-time and semiquantitative RT-PCR was done as previously described (Lim and Kai, 2007) with total RNA extracted from testes. Primer sequences are available in Table S1.

Real-Time RT-PCR for MicroRNA

Primers sequences are available in Table S1. Products were amplified from 100 ng of total RNA with the NCode miRNA First Strand cDNA Synthesis and qRT-PCR kits (Invitrogen) and quantitative PCR machine. The fold induction of miRNA was calculated relative to reference *miR-3*.

Chromatin Immunoprecipitation

ChIP was performed using the ChIP assay kit (Millipore) according to the manufacturers' manual with minor modifications. Ovaries dissected from 120 females of each genotype were used for one assay. Chromatin was cross-linked to proteins by 1% formaldehyde. Lysates were incubated overnight at 4°C with anti-FLAG (1:100, Sigma), anti-HP1 (1:50, DSHB), or anti-H3K9me3 (1:100, Upstate). DNA was recovered by phenol/ethanol extraction and ethanol precipitated. 1 μl of total 20 μl of DNA was used for PCR for 30–40 cycles. The amplified DNA was separated on 1.5% agarose gel and visualized with ethidium bromide. Primer sequences are available in Table S1.

Quantitative Western Blot

Testes from 10 males were dissected in Grace's medium and homogenized in sodium dodecyl sulfate (SDS)-sample buffer. Two-testes equivalent amount of supernatant was loaded per well of 10% SDS polyacrylamide gels. After electrophoresis, western blotting was done using standard protocols and probed rabbit anti-GFP (1:1,000; Molecular Probes) and mouse anti-alpha tubulin (1:200, Upstate). Infrared secondary antibodies were anti-rabbit (800 nm) and anti-mouse (680 nm), and were detected by an Odyssey infrared imaging system (LI-COR).

Statistical Analyses

Statistical analyses were done using Student's two-tailed t test assuming equal variance.

SUPPLEMENTAL DATA

Supplemental Data include six figures and one table and can be found with this article online at http://www.cell.com/developmental-cell/supplemental/S1534-5807(09)00301-3.

ACKNOWLEDGMENTS

We thank A. Nakamura, C.M. Field, D. McKearin, P. Lasko, R. Carthew, S. Hou, S. Cohen, the Developmental Studies Hybridoma Bank, and the Bloomington and Kyoto Stock Centers for reagents and fly stocks. We thank T. Ito and his group for technical support for ChIP experiments. We also thank W. Chia and S. Cohen for critical reading of the manuscript, and the Kai laboratory members L. Tao, V. Partil, and J. Honda for discussion and help with experiments. A.K.L. generated the anti-Mael antibody and contributed to ovary staining in Figures S3A–3D. J.W.P. performed all remaining analysis. J.W.P. and T.K. interpreted the data and wrote the paper. A.K.L. is supported by a fellowship from the Singapore Millennium Foundation program. This work is supported by Temasek Lifesciences Laboratory and the Singapore Millennium Foundation.

Received: March 10, 2009
Revised: June 10, 2009
Accepted: July 28, 2009
Published: September 14, 2009

REFERENCES

Aboobaker, A.A., Tomancak, P., Patel, N., Rubin, G.M., and Lai, E.C. (2005). *Drosophila* microRNAs exhibit diverse spatial expression patterns during embryonic development. Proc. Natl. Acad. Sci. USA *102*, 18017–18022.

Aravin, A.A., Lagos-Quintana, M., Yalcin, A., Zavolan, M., Marks, D., Snyder, B., Gaasterland, T., Meyer, J., and Tuschl, T. (2003). The small RNA profile during *Drosophila melanogaster* development. Dev. Cell *5*, 337–350.

Beest, M., Dooijes, D., Wetering, M., Kjaerulff, S., Bonvin, A., Nielsen, O., and Clevers, H. (2000). Sequence-specific High Mobility Group Box factors recognize 10–12 base pair minor groove motifs. J. Biol. Chem. *275*, 27266–27273.

Brawley, C., and Matunis, E. (2004). Regeneration of male germline stem cells by spermatogonial dedifferentiation in vivo. Science *304*, 1331–1334.

Brennecke, J., Hipfner, D.R., Stark, A., Russell, R.B., and Cohen, S.M. (2003). bantam encodes a developmentally regulated microRNA that controls cell proliferation and regulates the proapoptotic gene *hid* in *Drosophila*. Cell *113*, 25–36.

Brennecke, J., Stark, A., Russell, R.B., and Cohen, S.M. (2005). Principles of microRNA–target recognition. PLoS Biol. *3*, e85.

Brennecke, J., Aravin, A.A., Stark, A., Dus, M., Kellis, M., Sachidanandam, R., and Hannon, G.J. (2007). Discrete small RNA-generating loci as master regulators of transposon acitivity in *Drosophila*. Cell *128*, 1089–1103.

Bushati, N., and Cohen, S.M. (2007). microRNA functions. Annu. Rev. Cell Dev. Biol. *23*, 175–205.

Chen, D., and McKearin, D. (2003). Dpp signaling silences *bam* transcription directly to establish asymmetric divisions of germline stem cells. Curr. Biol. *13*, 1786–1791.

Cheng, J., Türkel, N., Hemati, N., Fuller, M.T., Hunt, A.J., and Yamashita, Y.M. (2008). Centrosome misorientation reduces stem cell division during ageing. Nature *456*, 599–604.

Costa, Y., Speed, R.M., Gautier, P., Semple, C.A., Maratou, K., Turner, J.M.A., and Cooke, H.J. (2006). Mouse MAELSRTROM: the link between meiotic silencing of unsynapsed chromatin and microRNA pathway? Hum. Mol. Genet. *15*, 2324–2334.

de Cuevas, M., and Spradling, A.C. (1998). Morphogenesis of the *Drosophila* fusome and its implication for oocyte specification. Development *125*, 2781–2789.

Eddy, E.M. (1975). Germ plasm and the differentiation of the germ cell line. Int. Rev. Cytol. *43*, 229–281.

Findley, S.D., Tamanaha, M., Clegg, N.J., and Ruohola-Baker, H. (2003). *Maelstrom*, a *Drosophila spindle*-class gene, encodes a protein that colocalizes with Vasa and RDE1/AGO1 homolog, Aubergine, in nuage. Development *130*, 859–871.

Forstemann, K., Tomari, Y., Du, T., Vagin, V.V., Denli, A.M., Bratu, D.P., Klattenhoff, C., Theurkauf, W.E., and Zamore, P.D. (2005). Normal microRNA maturation and germ-line stem cell maintenance requires Loquacious, a double-stranded RNA-binding domain protein. PLoS Biol. *3*, e236.

Fuller, M.T. (1993). Spermatogenesis. In The Development of *Drosophila melanogaster*, A. Martinez-Arias, ed. (Cold Spring Harbor: Cold Spring Harbor Press), pp. 71–147.

Fuller, M.T., and Spradling, A.C. (2007). Male and female *Drosophila* germline stem cells: two versions of immortality. Science *316*, 402–404.

Gonczy, P., Matunis, E., and DiNardo, S. (1997). *bag-of-marbles* and *benign gonial cell neoplasm* act in the germline to restrict proliferation during *Drosophila* spermatogenesis. Development *124*, 4361–4371.

Griffiths-Jones, S. (2004). The microRNA registry. Nucleic Acids Res. *32*, D109–D111.

Hatfield, S.D., Shcherbata, H.R., Fischer, K.A., Nakahara, K., Carthew, R.W., and Ruohola-Baker, H. (2005). Stem cell division is regulated by the microRNA pathway. Nature *435*, 974–978.

Jin, Z., and Xie, T. (2007). Dcr-1 maintains *Drosophila* ovarian stem cells. Curr. Biol. *17*, 539–544.

Kai, T., and Spradling, A. (2003). An empty *Drosophila* stem cell niche reactivates the proliferation of ectopic cells. Proc. Natl. Acad. Sci. USA *100*, 4633–4638.

Kai, T., and Spradling, A. (2004). Differentiating germ cells can revert into functional stem cells in *Drosophila melanogater* ovaries. Nature *428*, 564–569.

Kiger, A.A., White-Cooper, H., and Fuller, M.T. (2000). Somatic support cells restrict germline stem cell self-renewal and promote differentiation. Nature *407*, 750–754.

Klattenhoff, C., and Theurkauf, W. (2008). Biogenesis and germline functions of piRNAs. Development *135*, 3–9.

Kotaja, N., and Sassone-Corsi, P. (2007). The chromotoid body: a germ-cell-specific RNA-processing center. Nat. Rev. Mol. Cell Biol. *8*, 85–90.

Leatherman, J.L., and DiNardo, S. (2008). *Zfh-1* controls somatic stem cell self-renewal in the *Drosophila* testis and nonautonomously influences germline stem cell self-renewal. Cell Stem Cell *3*, 44–54.

Li, X., and Carthew, R.W. (2005). A microRNA mediates EGF receptor signaling and promotes photoreceptor differentiation in the *Drosophila* eye. Cell *123*, 1267–1277.

Lim, A.K., and Kai, T. (2007). Unique germ-line organelle, nuage, functions to repress selfish genetic elements in *Drosophila melanogaster*. Proc. Natl. Acad. Sci. USA *104*, 6714–6719.

McKearin, D.M., and Spradling, A.C. (1990). *bag-of-marbles:* a *Drosophila* gene required to initiate both male and female gametogenesis. Genes Dev. *4*, 2242–2251.

Nakagawa, T., Nabeshima, Y., and Yoshida, S. (2007). Functional identification of the actual and potential stem cell compartments in mouse spermatogenesis. Dev. Cell *12*, 195–206.

Neumüller, R.A., Betschinger, J., Fischer, A., Bushati, N., Poernbacher, I., Mechtler, K., Cohen, S.M., and Knoblich, J.A. (2008). Mei-P26 regulates microRNAs and cell growth in the *Drosophila* ovarian stem cell lineage. Nature *454*, 241–245.

Ohlstein, B., and McKearin, D. (1997). Ectopic expression of the *Drosophila* Bam protein eliminates oogenic germline stem cells. Development *124*, 3651–3662.

Pane, A., Wehr, K., and Schupbach, T. (2007). *zucchini* and *squash* encode two putative nucleases required for rasiRNA production in the *Drosophila* germline. Dev. Cell *12*, 851–862.

Park, J.K., Liu, X., Strauss, T.J., McKearin, D.M., and Liu, Q. (2007). The miRNA pathway intrinsically controls self-renewal of *Drosophila* germline stem cells. Curr. Biol. *17*, 533–538.

Pepling, M.E., Cuevas, M., and Spradling, A.C. (1999). Germline cysts: a conserved phase of germ cell development? Trends Cell Biol. *9*, 257–262.

Rorth, P., Szabo, K., Bailey, A., Laverty, T., Rehm, J., Rubin, G.M., Weigmann, K., Milan, M., Benes, V., Ansorge, W., and Cohen, S.M. (1998). Systematic gain-of-function genetics in *Drosophila*. Development *125*, 1049–1057.

Sarkar, A., Parikh, N., Hearn, S.A., Fuller, M.T., Tazuke, S.I., and Schulz, C. (2007). Antagonistic roles of Rac and Rho in organizing the germ cell microenvironment. Curr. Biol. *17*, 1253–1258.

Singh, S.R., and Hou, S.X. (2008). Immunohistological techniques for studying the *Drosophila* male germline stem cell. Methods Mol. Biol. *450*, 45–59.

Song, X., Wong, M.D., Kawase, E., Xi, R., Ding, B.C., McCarthy, J.J., and Xie, T. (2004). Bmp signals from niche cells directly repress transcription of a differentiation-promoting gene, *bag of marbles*, in germline stem cells in the *Drosophila* ovary. Development *131*, 1353–1364.

Soper, S.F.C., Heijden, G.W., Hardiman, T.C., Goodheart, M., Martin, S.L., Boer, P., and Bortvin, A. (2008). Mouse Maelstrom, a component of nuage, is essential for spermatogenesis and transposon repression in meiosis. Dev. Cell *15*, 285–297.

Stark, A., Brennecke, J., Russell, R.B., and Cohen, S.M. (2003). Identification of *Drosophila* microRNA targets. PLoS Biol. *1*, E60.

Tracey, W.D., Jr., Ning, X., Klingler, M., Kramer, S.G., and Gergen, J.P. (2000). Quantitative analysis of gene function in the *Drosophila* embryo. Genetics *154*, 273–284.

Tran, J., Brenner, T.J., and DiNardo, S. (2000). Somatic control over the germline stem cell lineage during *Drosophila* spermatogenesis. Nature *407*, 754–757.